Ligands influence a carbon nanotube penetration through a lipid bilayer

Citation: Liu, Fei, Dan Wu, and Ken Chen. "Ligands influence a carbon nanotube penetration through a lipid bilayer." Journal of Nanoparticle Research November 2014, 16:2692.

As Published: http://dx.doi.org/10.1007/s11051-014-2692-8

Publisher: Springer Netherlands

Persistent URL: http://hdl.handle.net/1721.1/103365

Version: Author's final manuscript: final author's manuscript post peer review, without publisher's formatting or copy editing

Ligands influence a carbon nanotube penetration through a lipid bilayer

Fei LIU[1,2], Dan WU[3] , Ken CHEN[3]

1. State Key Laboratory of Mechanical Transmission, College of Mechanical Engineering, Chongqing University, Chongqing, China

2. Departments of Biological Engineering, Massachusetts Institute of Technology, Cambridge, USA

3. Department of Mechanical Engineering, Tsinghua University, Beijing, China

***Corresponding Author**

Fei Liu

Address: Room 315-2, Teaching Building 7,

Chongqing University, Chongqing, 400044,China

Tel:+86-13101328216

E-mail: liufei09@mit.edu

Abstract

The interactions between nanomaterials and biological membranes are important for the safe use of nanomaterials. We explore the nano-bio interface by studying the penetration of a carbon nanotube (CNT) coated with ligands through a lipid bilayer. With a dissipative particle dynamics model, the mechanism of ligands influencing nano-bio interaction is analyzed. The CNTs with different ligands are tested. The simulation shows that the increase of the total number of ligand particles decreases the capability of a CNT penetrating through a membrane. For the CNTs with the same number of ligand particles, the arrangements of their ligands determine their behaviors. The asymmetrical pattern generates an upside down phenomenon, which requires more energy to get through the membrane; the uniform distribution penetrates through a membrane with less difficulty. Decreasing the stiffness, the length of ligands or preferring hydrophobic ligands increase the penetration capability of CNTs.

Keywords: lipid bilayer; carbon nanotube; functionalized ligands

1. Introduction

Nanotechnology has made astonishing progress and been widely discussed during the past decades. The nanoscale structures, such as nanoparticles, carbon nanotubes (CNTs), nanoprobes and fullerenes are extensively used in many fields, such as optics, sensing, electronics, and material science. As the development of biology, recent studies also focus on the nanostructures' applications in biomedical engineering, including drug delivery(Mei et al. 2013; Park 2013), gene therapy(Bahadur et al. 2014; Hwang et al. 2014), and diagnostics(Young and Kairdolf 2013). In these biomedical applications, functionalized nanostructures are required to penetrate into the eukaryotic or prokaryotic cells(Shreekumar 2012; Verma and Stellacci 2010). However, when penetrating the biological cells, the engineered nanostructures may interact with some unexpected biological molecules which could have bio-compatible or bio-adverse outcomes(Nel et al. 2009). Therefore, the interface between the nanostructure and the bio-system has generated great interest in the past years(Gagner et al. 2012; Nel et al. 2009).

In general, the nano-bio interface comprises physical, chemical and biological interactions(Nel et al. 2009). The main biophysicochemical influences can be divided into four parts: 1) the structure of the nanomaterials, such as size, shape, ligands, hydrophobicity and hydrophilicity; 2) the properties of the suspending media, including acids, bases, salts and multivalent ions; 3) solid-liquid interface, for example the surface hydration and dehydration, the surface reconstruction and the release of free surface energy; 4) biological interaction: receptor-ligand binding interaction, membrane wrapping, and oxidant injury to biomolecules, etc.(Nel et al. 2009). Moreover, these influences are not independent but highly coupled, which tremendously increases the difficulty of understanding the interactions between the nanomaterials and bio-system. Therefore, though quite important, the nano-bio interface is poorly understood at present.

It may be impossible to describe all these biophysicochemical interactions clearly at one time, but scientists have provided some conceptual frameworks and successfully analyzed the influences one by one, separately. For example, when the functionalized nanostructures enter a biological cell, the cell membrane would prevent the entrance of these foreign materials. Some researchers have studied the interaction between the nanostructure and the lipid bilayer to reveal the nano-bio interface(Donkor and Tang 2014; Liu et al. 2013b; Sarukhanyan et al. 2014). Yang and Ma investigated nanoparticles with different shapes/volumes across a lipid bilayer(Yang and Ma 2010). They found that the shape anisotropy and initial orientation of nanoparticles were important to the nano-bio interfaces. Kraszewski and his colleges claimed that the ability of a CNT passing through a lipid bilayer was a function of the CNT's length.(Kraszewski et al. 2012) Their data proved that short nanotubes could passively penetrate the bilayer. Our previous work analyzed the interaction between a nanoprobe and a lipid bilayer, especially how the surface property of a nanoprobe affected the interface(Liu et al. 2013a). We found that a hydrophilic nanoprobe generated a hydrophilic hole while a hydrophobic probe leaded to a 'T-junction' scenario when penetrating a membrane. The transfer of fullerenes at nano-scales into lipid bilayers were reported by Jusufi with molecular dynamics(Jusufi et al. 2011). He tested C60, C180 and C540, and proposed free energy profiles during transferring to confirm the spontaneous absorption of all the three fullerenes. Some experimental studies have shown that the ligands functioned on the nanostructures can influence the nano-bio interface (Tan et al. 2010; Verma et al. 2008), but the mechanism is poorly studied. In this paper, we will focus on the influences of the coated ligands on the nano-bio interface. Considering the well-organized geometrical structure of CNTs, the CNT coated with ligands is selected as an example to promote our studies. As one of the representative products in nanoscience, the CNT has been widely studied for more than 20 years since it was discovered by Iijima in 1991(Iijima 1991). It is an effective tool

for various biomedical applications(Fabbro et al. 2013; Liu et al. 2009; Yang et al. 2007). In such applications, CNTs usually are coated with some target ligands (Esser et al. 2012; Münzer et al. 2014; Moser et al. 2014; Ormsby et al. 2014). The mechanism that these ligands influence the nano-bio interface will be discussed in this paper.

2. Method and model

The lipid bilayer is made of two lipid leaflets with hydrophilic 'heads' on the surfaces and hydrophobic 'tails' in the core. Dissipative particle dynamics (DPD) is a coarse grained computer simulation method extensively applied to study bio-membrane systems(Ganzenmüller et al. 2011; Goetz and Lipowsky 1998; Goicochea 2014; Peng et al. 2014).

2.1 Dissipative particle dynamics

DPD is utilized to analyze the interaction between a CNT and a lipid bilayer. In DPD, different kinds of molecules are represented by different types of coarse grained particles. There are three types of interactive forces between two particles: a conservative force, a dissipative force and a random force. The three repulsive forces work together to determine the motions of the particles. The conservative force between two particles i and j is

$$\mathbf{F}_{ij}^{C} = \begin{cases} a_{ij}(1 - r_{ij}/r_0)\hat{\mathbf{r}}_{ij} & r_{ij} \le r_0 \\ 0 & r_{ij} > r_0 \end{cases} \tag{1}$$

where a_{ij} is the conservative force parameter determined by the types of interactive-pair particles. It represents the maximum repulsive force between particle i and j. The larger a_{ij} is, the larger repulsive force between particle i and j. The a_{ij} between other type of particle and the water particle can represent hydrophilicity/ hydrophobicity of this type of particle. The larger a_{ij}, the more hydrophobic. r_{ij} is the distance between particles i and j, with $\hat{\mathbf{r}}_{ij}$ as the unit vector from particle j to

i. r_0 is the cut-off radius, and also the length unit in DPD (Illya et al. 2005). If $r_{ij} > r_0$, the conservative force is zero.

The dissipative force is a drag force between a pair of particles which is a linear function of their relative momentum. It works together with random force to simulate the fluctuation and form a thermostat so as to keep the system at a constant temperature (Espanol and Warren 1995; Groot and Warren 1997).

$$\mathbf{F}_{ij}^{D} = \begin{cases} \gamma_{ij}\omega_{ij}^{D}(\hat{\mathbf{r}}_{ij}\cdot\mathbf{v}_{ij})\hat{\mathbf{r}}_{ij} & r_{ij} \le r_0 \\ 0 & r_{ij} > r_0 \end{cases} \tag{2}$$

where γ_{ij} is the dissipative force parameter between particle i and j, and $\mathbf{v}_{ij} = \mathbf{v}_i - \mathbf{v}_j$ is the relative velocity vector. ω_{ij}^{D} is the dissipative weighting function depending on r_{ij}, $\omega_{ij}^{D} = (1 - r_{ij}/r_0)^2$ (Espanol and Warren 1995) .

The random force between particles i and j is

$$\mathbf{F}_{ij}^{R} = \begin{cases} \sigma_{ij}\omega_{ij}^{R}\theta_{ij}\dfrac{1}{\sqrt{\Delta t}}\hat{\mathbf{r}}_{ij} & r_{ij} \le r_0 \\ 0 & r_{ij} > r_0 \end{cases} \tag{3}$$

where σ_{ij} is the random force parameter, ω_{ij}^{R} is the random weighting function described as $\omega_{ij}^{R} = (1 - r_{ij}/r_0)$ (Espanol and Warren 1995). θ_{ij} is a fluctuating variable following Gaussian distribution with zero mean and unit variance. Δt is the time of per simulation step. The dissipative force parameter (Eq. 2) and the random force parameter (Eq. 3) follow the relation $\sigma_{ij}^2 = 2\gamma_{ij}k_B T$, where k_B is Boltzmann constant, T is the Kelvin temperature. The most accepted values $\sigma_{ij} = 3$ and $\gamma_{ij} = 4.5$, $T = 300K$ are used in our simulation(Ortiz et al. 2005).

2.2 Membrane model

We introduce hydrophilic head particles (*H*) and hydrophobic tail particles (*T*) to

simulate the lipid molecules in a lipid bilayer. The structure of a chain lipid molecule is described as $H_3(T_4)_2$, Fig.1c, corresponding to the physical structure of a phospholipid bilayer. Water particles (*W*) are located randomly around the lipid bilayer molecules at the initial state.

In a chain lipid molecule, the two adjacent particles are linked with a Hookean spring and the elastic force is

$$\mathbf{F}_{ij}^{s} = k_s(r_{ij} - r_{eq})\hat{\mathbf{r}}_{ij} \tag{4}$$

where particle i and j are adjacent particles in a chain lipid molecule (Fig.1c), and r_{eq} is the equilibrium bond length with $r_{eq} = 0.5r_0$. k_s is the extension stiffness with the value 128(Gao et al. 2007).

The three-body potential among adjacent particle triples (Fig.1c) in a lipid molecule is used to calculate the hydrocarbon chain stiffness.

$$U_{\varphi(i-1,i,i+1)} = k_\varphi(1-\cos(\varphi-\varphi_0)) \tag{5}$$

where $U_{\varphi(i-1,i,i+1)}$ is the three-body potential, and φ is the angle defined by the adjacent particle triples $i-1$, i and $i+1$; φ_0 is the equilibrium angle with $\varphi_0 = 0$; k_φ is the bending stiffness valued as 20(Gao et al. 2007). The bond-bending force is

$$\mathbf{F}_{(i-1,i,i+1)}^{\varphi} = -\nabla U_{\varphi(i-1,i,i+1)} \tag{6}$$

The simulation space is $32\times32\times32r_0^3$ with 1600 $H_3(T_4)_2$ lipid molecules and 82000 *W* particles. The value of a_{ij} between a water particle and another type of particle defines the hydrophilicity/hydrophobicity of this type of particle: the larger a_{ij}, the more hydrophobic the particle. We set : $a_{HH} = 25$, $a_{HT} = 50$, $a_{HW} = 35$; $a_{TT} = 25$, $a_{TW} = 75$; $a_{WW} = 25$ (the subscripts indicate the types of particles)(Gao et al. 2007). Periodic boundary conditions are applied in all three dimensions to minimise the edge

effects(Groot and Warren 1997). After 30,000 simulation steps, the three types of particles are assembled into a planar bilayer presented in Fig. 1a, with H particles arranged on the two surfaces of the lipid bilayer, T particles in the core, and the surrounding W particles are not drawn for clarity. The lipid bilayer structure in Fig. 1a agrees well with that of a classical lipid bilayer. By comparing the physical thickness of cell membrane (5-6 nm) and the diffusion coefficient of lipid bilayer ($5\mu m^2/s$) with the corresponding values in DPD model, we obtain the length unit in simulation model $r_0 \approx 0.7$ nm and the time of per simulation step $\Delta t \approx 7.4$ps (Illya et al. 2005).

2.3 Carbon nanotube model

An armchair nanotube with the chirality (10, 10) is selected in our model. The diameter of the carbon nanotube is ~ 1.5nm, and the aspect ratio is 2.5, Fig. 1b. It can float and rotate freely during simulation with its shape is fixed. To simulate the ligands' infulence, we coated some stripes on the nanotube. The striped nanostructures have been found on sphere nanoparticle by Francesco Stellacci's group (Cho et al. 2012; Jackson et al. 2004; Liu et al. 2012; Moglianetti et al. 2014; Verma et al. 2008) , ellipsoidal nanoparticles by Craig J. Hawker and coworkers (Jang et al. 2013), and nanoprobes by Nicholas A. Melosh (Almquist et al. 2011). Their works make us believe that the striped nanotube is possible in the realistic experimental systems. In our nanotube model, ligand particles (L) are introduced to simulate the ligands coated on the nanotubes, Fig.1b. The ligand patterns are described as $[M, N, Q]$. M is the number of layers of coated ligands; N is the number of ligands on each layer; Q shows the number of particles of each ligand. For example, the ligand pattern in Fig.1b is [8, 5, 4] which means there are eight layers of coated ligands, on each layer there are five ligands, and each ligand is composed of four particles, Fig.1b. The adjacent L particles in a ligand are connected, and $k_{ligand} = [k_s^{ligand}, k_\varphi^{ligand}]$ defines the stiffness of

ligands. k_s^{ligand} is the extension stiffness of ligands and k_φ^{ligand} is the bending stiffness. The first L particle in each ligand is connected with the selected CNT particle with a zero initial distance to ensure the ligand arrangement, and the connection stiffness is the same with that between two L particles in a ligand, Fig 1b. a_{LH}, a_{LT}, a_{LW} are the conservative force parameters between L particles and H, T, W particles respectively. a_{LH}, a_{LT}, a_{LW} determine the hydrophilicity/hydrophobicity of a ligand. The length of a ligand (r_{ligand}) is defined as the distance between the two adjacent ligand particles, Fig.1b.

The CNT is placed at the center of the lipid bilayer, and the bottom of the CNT is located $2r_0$ above the membrane in the initial state, Fig.1a. Under these initial conditions there is no interaction between the ligands and the membrane. An eighth of the CNT is colored in blue to show its rotation in penetration (Fig.1b). At the initial condition, we set $k_{ligand} = k_0$, where $k_0 = [k_s, k_\varphi]$, $r_{ligand} = 0.25r_0$, $a_{LH} = 15$, $a_{LT} = 75$, $a_{LW} = 35$, which illustrates a hydrophilic ligand pattern with medium stiffness and length. These values are used throughout our discussions if no specification is declared.

2.3 Driving force

Because of the 'hydrophilic-hydrophobic-hydrophilic' structure, a lipid bilayer behaves as a formidable barrier to most of the foreign materials. Therefore, an external force is usually required to push the nanostructure across the bilayer (Chen et al. 2007; Obataya et al. 2005). According to the literature, the minimum force describes the penetration capability of the nanostructure(Yang and Ma 2010). Thus, the minimum required driving force (F) is used to represent the penetration capability of a CNT. The smaller driving force a CNT requires, the easier it penetrates. During the calculation,

the bilayer is relaxed for 10,000 simulation steps (or $0.74\mu s$) with the CNT fixed at first.Then the CNT is released, and a downwards driving force F is generated at the same time. The force is added equally to all the CNT particles, so F can be treated as working at the center of the CNT. It pushes the CNT penetrating a lipid bilayer.

3. Results and discussions

The properties of ligands mainly include the number of ligand particles, the pattern of the ligands, the stiffness, length and hydrophilicity/hydrophobicity of ligands. In this section, we will discuss their influences on the penetrations.

3.1 Number of ligand particles

The morphologies of a lipid bilayer penetrated by four CNTs coated with different number of ligands are simulated, Fig. 2. The patterns of these CNTs are [2, 5, 4], [2, 10, 4], [2, 16, 4] ,[2, 20, 4] with medium hydrophilic ligands, corresponding to the total number of ligand particles 40, 80, 128, 160. All the four patterns have two layers of ligands with one layer located at the bottom of the CNTs while the other at the center. This arrangement makes the CNTs be asymmetrical in vertical direction: the bottoms of these CNTs are more hydrophilic than the tops. Figure 2 shows that the four CNTs behave similarly in penetration. After the CNTs are released, the hydrophilic ligand particles attract the lipid heads, and the driving forces push the CNTs to the lipid membrane, Fig.2 (2). As the CNTs go down, the hydrophobic tails in the lipid bilayer turn to dominate the interactions. The repulsive forces between the ligands and the tails make the CNTs upside down, Fig.2 (3). Because of the strong driving force, the CNTs overcome the prevention of the hydrophobic tails and pass through the membrane successfully, Fig.2 (4). When the CNTs are in the membrane, their ligands attract the hydrophilic heads and lead to hydrophilic holes around the CNTs, Fig.2a(4), which is observed in the previous research in nanoprobes(Liu et al. 2013a).

Though the four CNTs behave closely during penetration, their minimum driving forces required are different. In our model, the driving force is determined by at least 20 independent simulations in computation. In each simulation, a driving force is tested for 7.4μs (or 100,000 simulation steps). The driving force is determined by the following rules. Provided that one CNT never get through the membrane when $F < 51.2$ and always penetrates successfully with $F > 55.4$ within 100,000 steps, we set the driving force as $[51.2, 55.4]$. Figure 3 presents the driving force of each CNT. It indicates that the more number of ligand particles a CNT owns, the larger driving force it needs. Thus, the CNT with less ligand has a higher penetration capacity.

3.2 Arrangements of ligands

The upside down behaviors in Fig. 2 let us doubt the patterns or the arrangements of the ligands may influence the nano-bio interface. Therefore, three more patterns [4, 10, 4], [5, 8, 4], [8, 5, 4] are simulated. Adding the [2, 20, 4] pattern, the four patterns have the same number of the ligand particles (160 particles in total), but are different in ligand arrangements, Fig.2c, Fig.4. The [2, 20, 4], [4, 10, 4]and [5, 8, 4] patterns are asymmetrical in vertical while the [8, 5, 4] are symmetrical. Figure 4b shows that the symmetrical pattern does show a hydrophilic hole which is also found in the other three CNTs, but there is no upside down phenomenon of the [8, 5, 4] pattern which is observed in [2, 20, 4], [5, 8, 4] and [4, 10, 4] patterns. These results demonstrate that the arrangements of the ligands can affect the behaviors of the CNTs in a lipid bilayer.

Besides the behaviors of the lipid bilayers, we also calculate the driving forces of the four CNTs. In Fig.5, the [8, 5, 4] pattern penetrates with the smallest driving force while [2, 20, 4] requires the largest. Comparing the behaviors of the four CNTs in the membrane, we find that the asymmetrical patterns need to rotate their postures to adjust the lipid bilayer structure which costs some additional work; while the uniform

distribution patterns without rotation require less work. Therefore, we conclude that the uniform distribution of the ligands leads to a small driving force.

3.3 Ligand stiffness

In different experiments, different types of ligands may be used. These ligands could be different in stiffness, length and hydrophilic/hydrophobicity. To analyze the ligand stiffness influences on the nano-bio interface, different values of k_{ligand} are simulated. The driving forces of the [8, 5, 4] CNTs with different stiffnesses ligands are shown in Fig.6. Driving by the fluctuations, the flexible ligands are easier than the stiff ones to reshape themselves to adjust the membrane structure. Figure 6 shows that stiffer ligands require larger driving forces, due to the soft ligands can rearrange themselves into homogeneous patterns so as to enhance permeation(Gkeka et al. 2013).

3.4 Ligand length

The ligand length should be another influence. Here we analyze the ligand length influence by verifying the distance between two adjacent ligand particles, but not by changing the number of particles of each ligand. Because the former strategy can study the ligand length effect independently, while the latter changes the total number of ligand particles which could influence the interface (see section 3.1). Five CNTs with $r_{ligand} = 0.1r_0$, $r_{ligand} = 0.15r_0$, $r_{ligand} = 0.25r_0$, $r_{ligand} = 0.5r_0$ and $r_{ligand} = r_0$ are simulated with ligand pattern [8, 5, 4], Fig.7. Comparing with Fig.2c and Fig.7a, b, it is clear that the CNTs with shorter ligands interact with less lipid molecules during penetration.

The driving forces of the five CNTs are shown in Fig. 8. Obviously, the shorter ligand length requires a smaller driving force. Considering the finding in nanoparticles that the penetrating capability of a nanoparticle crossing a lipid bilayer is determined by the contact area between a particle and a lipid bilayer, we believe the larger driving

force of a longer ligand length CNT is due to its larger contact area which could be observed in Fig.7a, b.

3.5 Ligand hydrophilicity and hydrophobicity

Hydrophilicity/hydrophobicity of nanostructures have been studied by some researchers(Liu et al. 2013a; Van Lehn and Alexander-Katz 2011). Here we ignore the hydrophilicity/hydrophobicity of the CNTs, but focus on the hydrophilicity/hydrophobicity of the ligands. Figure 9 shows the behavior of a [8, 5, 4] CNT coated with hydrophobic ligands ($a_{LH} = 75$, $a_{LT} = 15$, $a_{LW} = 50$). Compared with the hydrophilic pattern in Fig.4b, the two CNTs behave very different. In Fig.9, after the CNT is released, the tail particles are attracted to adhere along the CNT, whereas the lipid heads are pushed towards the water. There is no hydrophilic hole(Fig.4) around the hydrophobic CNT but a slightly "T-junction" is formed, Fig.9(4), which is also observed in hydrophobic nanoprobes(Liu et al. 2013a). The hydrophobic pattern has a higher penetration capacity, which suggests that hydrophobic ligands would be a better choice for the penetration of CNTs. This finding agrees with the previous work (Pogodin and Baulin 2010).

4. Conclusions

The interaction between nanomaterials and biological cells are shaped by a lot of physical, biological, chemical influences. We take CNTs coated with ligands as an example to explore the influence of ligands. With our DPD model, the physical chemical properties of ligands are analyzed. The simulations show that the less total number of ligand particles a CNT is coated with, the higher penetration capacity the CNT possesses. The hydrophilic ligands cause hydrophilic holes around CNTs while the hydrophobic ligands generate 'T junction' scenarios. For the CNTs with the same

number of ligand particles, the arrangements of the ligands influence the behaviors of CNTs. An upside down phenomenon is observed with an asymmetrical pattern, and the uniform distribution pattern penetrates the membrane with less difficulty. Decreasing the stiffness, the ligand length or preferring a hydrophobic ligand can increase the penetration possibility of CNTs. Our research should benefit the research of the nano-bio interface and provide some suggestions in designing an effective nanostructure to penetrate the cell membrane as well.

Acknowledgements

The authors would like to gratefully acknowledge the financial support for portions of this research from the Fundamental Research Funds for the Central Universities under Grant No. CDJZR14905502, the National Natural Science Foundation of China under Grant No. 51175278, and the Singapore-MIT Alliance for Research and Technology.

References

Almquist BD, Verma P, Cai W, Melosh NA (2011) Nanoscale patterning controls inorganic–membrane interface structure. Nanoscale 3(2):391-400.

Bahadur K, Thapa B, Bhattarai N (2014) Gold nanoparticle-based gene delivery: promises and challenges. Nanotechnology Reviews 3(3):269-280.

Chen X, Kis A, Zettl A, Bertozzi CR (2007) A cell nanoinjector based on carbon nanotubes. Proceedings of the National Academy of Sciences 104(20):8218-8222.

Cho ES, Kim J, Tejerina B, Hermans TM, Jiang H, Nakanishi H, Yu M, Patashinski AZ, Glotzer SC, Stellacci F (2012) Ultrasensitive detection of toxic cations through changes in the tunnelling current across films of striped nanoparticles. Nature materials 11(11):978-985.

Donkor DA, Tang XS (2014) Tube length and cell type-dependent cellular responses to ultra-short single-walled carbon nanotube. Biomaterials 35(9):3121-3131.

Espanol P, Warren P (1995) Statistical mechanics of dissipative particle dynamics. EPL (Europhysics Letters) 30:191.

Esser B, Schnorr JM, Swager TM (2012) Selective Detection of Ethylene Gas Using Carbon Nanotube‐based Devices: Utility in Determination of Fruit Ripeness. Angewandte Chemie International Edition 51(23):5752-5756.

Fabbro C, Ros TD, Prato M (2013) Carbon nanotube derivatives as anticancer drug delivery systems. Organic Nanomaterials: Synthesis, Characterization, and Device Applications:469-486.

Gagner JE, Shrivastava S, Qian X, Dordick JS, Siegel RW (2012) Engineering Nanomaterials for Biomedical Applications Requires Understanding the Nano-Bio Interface: A Perspective. The Journal of Physical Chemistry Letters 3(21):3149-3158.

Ganzenmüller G, Hiermaier S, Steinhauser M (2011) Shock-wave induced damage in lipid bilayers: a dissipative particle dynamics simulation study. Soft Matter 7(9):4307-4317.

Gao L, Shillcock J, Lipowsky R (2007) Improved dissipative particle dynamics simulations of lipid bilayers. The Journal of chemical physics 126:015101.

Gkeka P, Sarkisov L, Angelikopoulos P (2013) Homogeneous Hydrophobic–Hydrophilic Surface Patterns Enhance Permeation of Nanoparticles through Lipid Membranes. The Journal of Physical Chemistry Letters 4(11):1907-1912.

Goetz R, Lipowsky R (1998) Computer simulations of bilayer membranes: Self-assembly and interfacial tension. The Journal of chemical physics 108:7397.

Goicochea AG. 2014. Designing Biodegradable Surfactants and Effective Biomolecules with Dissipative Particle Dynamics. Experimental and Computational Fluid Mechanics: Springer. p 433-447.

Groot RD, Warren PB (1997) Dissipative particle dynamics: bridging the gap between atomistic and mesoscopic simulation. Journal of Chemical Physics 107(11):4423.

Hwang SR, Ku SH, Joo MK, Kim SH, Kwon IC (2014) Theranostic nanomaterials for image-guided gene therapy. MRS bulletin 39(01):44-50.

Iijima S (1991) Helical microtubules of graphitic carbon. nature 354(6348):56-58.

Illya G, Lipowsky R, Shillcock J (2005) Effect of chain length and asymmetry on material properties of bilayer membranes. The Journal of chemical physics 122:244901.

Jackson AM, Myerson JW, Stellacci F (2004) Spontaneous assembly of subnanometre-ordered domains

in the ligand shell of monolayer-protected nanoparticles. Nature materials 3(5):330-336.
Jang SG, Audus DJ, Klinger D, Krogstad DV, Kim BJ, Cameron A, Kim S-W, Delaney KT, Hur S-M, Killops KL (2013) Striped, Ellipsoidal Particles by Controlled Assembly of Diblock Copolymers. Journal of the American Chemical Society 135(17):6649-6657.
Jusufi A, DeVane RH, Shinoda W, Klein ML (2011) Nanoscale carbon particles and the stability of lipid bilayers. Soft Matter 7(3):1139-1146.
Kraszewski S, Picaud F, Elhechmi I, Gharbi T, Ramseyer C (2012) What length of functionalized carbon nanotubes can passively penetrate a lipid membrane? Carbon.
Liu F, Wu D, Kamm RD, Chen K (2013a) Analysis of nanoprobe penetration through a lipid bilayer. Biochimica et Biophysica Acta (BBA)-Biomembranes 1828(8):1667-1673.
Liu L, Yang C, Zhao K, Li J, Wu H-C (2013b) Ultrashort single-walled carbon nanotubes in a lipid bilayer as a new nanopore sensor. Nature communications 4.
Liu X, Yu M, Kim H, Mameli M, Stellacci F (2012) Determination of monolayer-protected gold nanoparticle ligand–shell morphology using NMR. Nature communications 3:1182.
Liu Z, Tabakman SM, Chen Z, Dai H (2009) Preparation of carbon nanotube bioconjugates for biomedical applications. Nature protocols 4(9):1372-1381.
Münzer AM, Seo W, Morgan GJ, Michael ZP, Zhao Y, Melzer K, Scarpa G, Star A (2014) Sensing Reversible Protein-ligand Interactions with Single-walled Carbon Nanotube Field-effect Transistors. The Journal of Physical Chemistry C.
Mei L, Zhang Z, Zhao L, Huang L, Yang X-L, Tang J, Feng S-S (2013) Pharmaceutical nanotechnology for oral delivery of anticancer drugs. Advanced drug delivery reviews 65(6):880-890.
Moglianetti M, Ong QK, Reguera J, Harkness KM, Mameli M, Radulescu A, Kohlbrecher J, Jud C, Svergun DI, Stellacci F (2014) Scanning tunneling microscopy and small angle neutron scattering study of mixed monolayer protected gold nanoparticles in organic solvents. Chemical Science 5(3):1232-1240.
Moser ML, Tian X, Pekker A, Sarkar S, Bekyarova E, Itkis ME, Haddon RC (2014) Hexahapto-lanthanide interconnects between the conjugated surfaces of single-walled carbon nanotubes. Dalton Transactions 43(20):7379-7382.
Nel AE, Mädler L, Velegol D, Xia T, Hoek EM, Somasundaran P, Klaessig F, Castranova V, Thompson M (2009) Understanding biophysicochemical interactions at the nano–bio interface. Nature materials 8(7):543-557.
Obataya I, Nakamura C, Han S, Nakamura N, Miyake J (2005) Nanoscale operation of a living cell using an atomic force microscope with a nanoneedle. Nano letters 5(1):27-30.
Ormsby RW, McNally T, Mitchell CA, Musumeci A, Schiller T, Halley P, Gahan L, Martin D, Smith SV, Dunne NJ (2014) Chemical modification of multiwalled carbon nanotube with a bifunctional caged ligand for radioactive labelling. Acta Materialia 64:54-61.
Ortiz V, Nielsen SO, Discher DE, Klein ML, Lipowsky R, Shillcock J (2005) Dissipative particle dynamics simulations of polymersomes. The Journal of Physical Chemistry B 109(37):17708-17714.
Park K (2013) Facing the truth about nanotechnology in drug delivery. ACS nano 7(9):7442-7447.
Peng Z, Pivkin IV, Li X, Karniadakis GE, Dao M (2014) Two-Component Dissipative Particle Dynamics Model of Red Blood Cells. Biophysical Journal 106(2):573a.

Pogodin S, Baulin VA (2010) Can a carbon nanotube pierce through a phospholipid bilayer? ACS nano 4(9):5293-5300.

Sarukhanyan E, De Nicola A, Roccatano D, Kawakatsu T, Milano G (2014) Spontaneous insertion of carbon nanotube bundles inside biomembranes: A hybrid particle-field coarse-grained molecular dynamics study. Chemical Physics Letters 595:156-166.

Shreekumar P (2012) Toxicity Issues Related to Biomedical Applications of Carbon Nanotubes. Journal of Nanomedicine & Nanotechnology.

Tan SJ, Jana NR, Gao S, Patra PK, Ying JY (2010) Surface-ligand-dependent cellular interaction, subcellular localization, and cytotoxicity of polymer-coated quantum dots. Chemistry of Materials 22(7):2239-2247.

Van Lehn RC, Alexander-Katz A (2011) Penetration of lipid bilayers by nanoparticles with environmentally-responsive surfaces: simulations and theory. Soft Matter 7(24):11392-11404.

Verma A, Stellacci F (2010) Effect of surface properties on nanoparticle–cell interactions. Small 6(1):12-21.

Verma A, Uzun O, Hu Y, Hu Y, Han H-S, Watson N, Chen S, Irvine DJ, Stellacci F (2008) Surface-structure-regulated cell-membrane penetration by monolayer-protected nanoparticles. Nature materials 7(7):588-595.

Yang K, Ma Y-Q (2010) Computer simulation of the translocation of nanoparticles with different shapes across a lipid bilayer. Nature nanotechnology 5(8):579-583.

Yang W, Thordarson P, Gooding JJ, Ringer SP, Braet F (2007) Carbon nanotubes for biological and biomedical applications. Nanotechnology 18(41):412001.

Young AN, Kairdolf BA (2013) Nanotechnology in molecular diagnostics. Molecular Genetic Pathology:383-398.

Figure Captions

Figure 1. (a) The DPD model used to simulate a CNT functioned with ligands penetrating through a lipid bilayer. (b) The $[8, 5, 4]$ ligand pattern, with eight layers of ligands, five ligands on each layer and four L particles (green) of each ligand. The blue part of the CNT is colored to show the rotation in penetration. (c) A lipid molecule $H_3(T_4)_2$ with three H particles (red) and eight T particles (yellow, arranged as two chains). The adjacent pairs connected with black lines experience linear elastic forces, and the linked triples are partially controlled by bond-bending forces.

Figure 2. The behaviors of the three CNTs coated with different number of ligands across a lipid bilayer. (a) Ligand pattern [2, 5, 4]; (b) Ligand pattern [2, 10, 4]; (c) Ligand pattern [2, 20, 4]. The three asymmetrical patterns show an upside down phenomenon. Hydrophilic holes are generated around the CNTs.

Figure 3. The driving forces of four CNTs coated with different number of ligand particles across a lipid layer. The CNT with more ligand particles has a lower penetration capacity.

Figure 4. The behaviors of the CNTs coated with different arrangements of ligands across a lipid bilayer. (a) Ligand pattern [4, 10, 4]; (b) Ligand pattern [8, 5, 4]. There is no upside down phenomenon observed for the symmetrical pattern [8, 5, 4].

Figure 5. The driving forces of the CNTs coated with the same number of ligands but different arrangements across a lipid layer. The uniform distribution expresses a higher penetration capacity.

Figure 6. The driving forces of the CNTs coated with ligands with different stiffnesses across a lipid layer. The softer the ligands are, the higher penetration capacity a CNT possesses.

Figure 7. The behaviors of the CNTs coated with ligands with different lengths across a lipid bilayer. (a) The ligand length $r_{ligand} = 0.1r_0$; (b) The ligand length $r_{ligand} = 0.5r_0$. The CNTs with shorter ligands have smaller contact areas than those with longer ligands.

Figure 8. The driving forces of the CNTs coated with ligands with different lengths

across a lipid bilayer. The decrease of the ligand length increases the penetration capacity of a CNT.

Figure 9. The behaviors of the CNT coated with hydrophobic ligands across a lipid bilayer. The hydrophobic pattern generated a “T- junction” instead of a hydrophilic hole when penetrating the membrane.

Figures

Figure 1

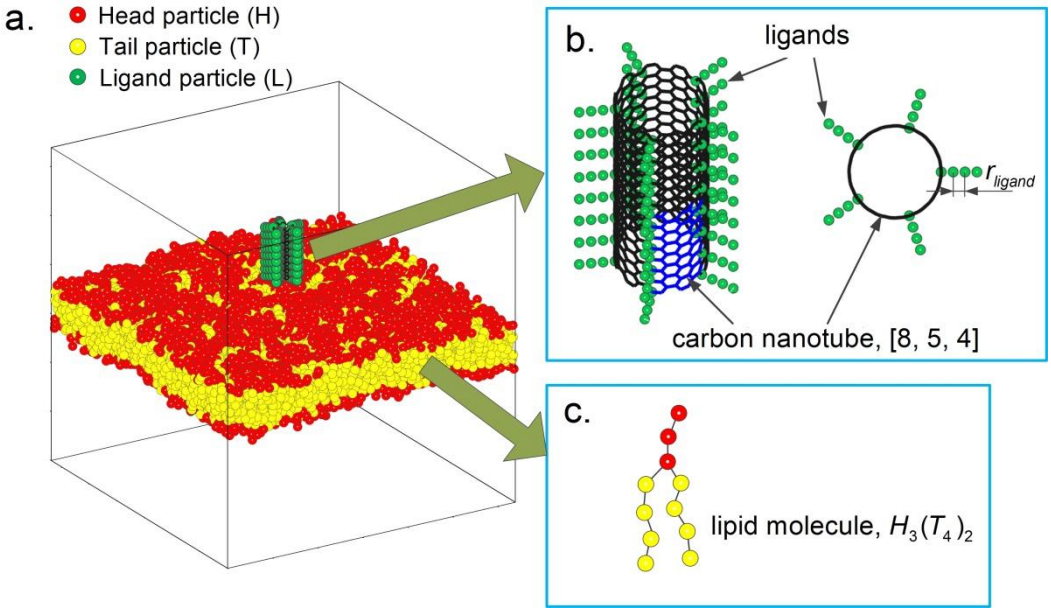

Figure 2

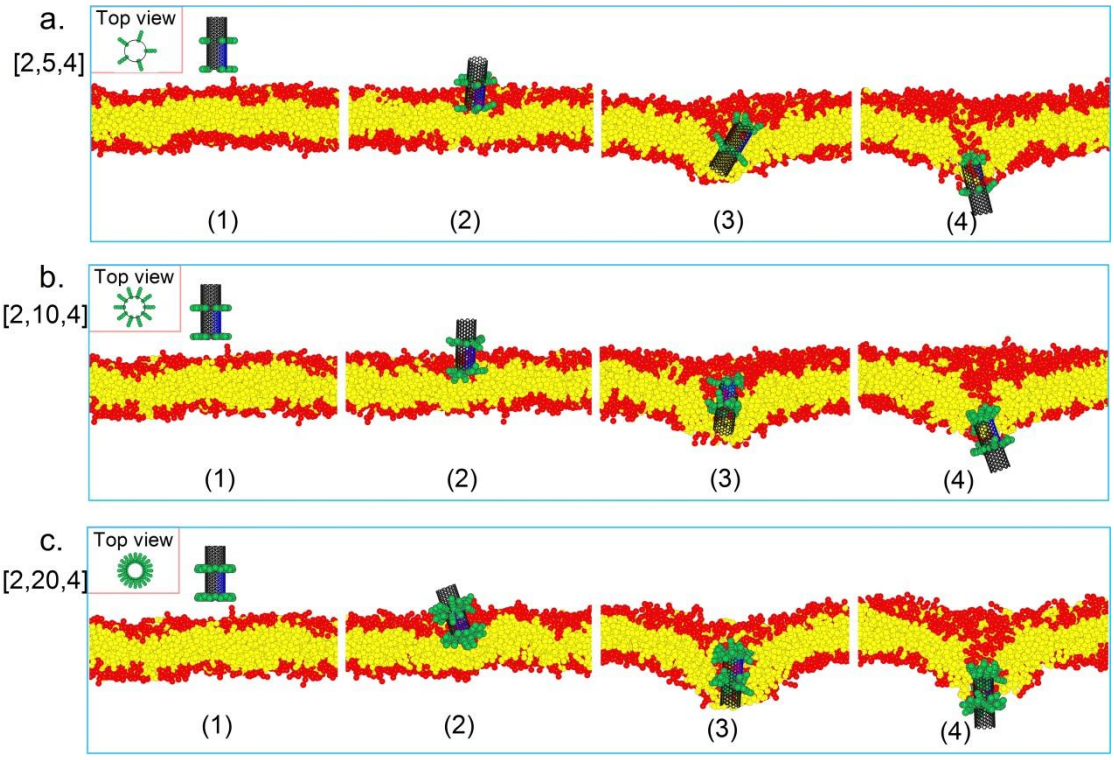

Figure 3

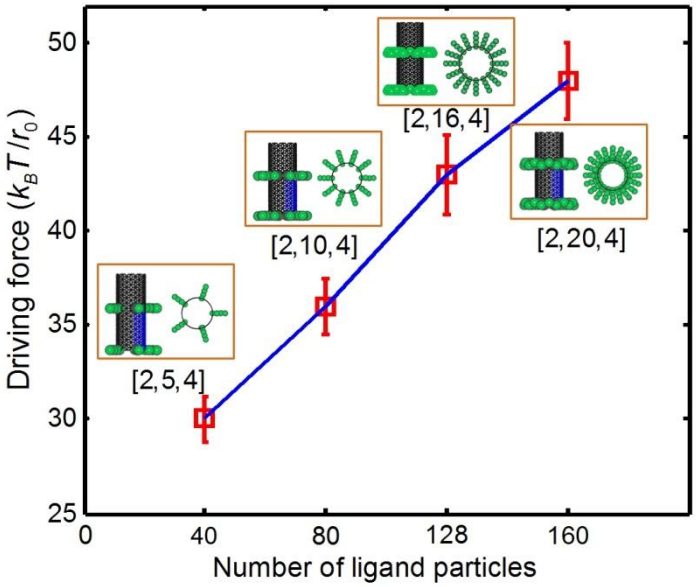

Figure 4

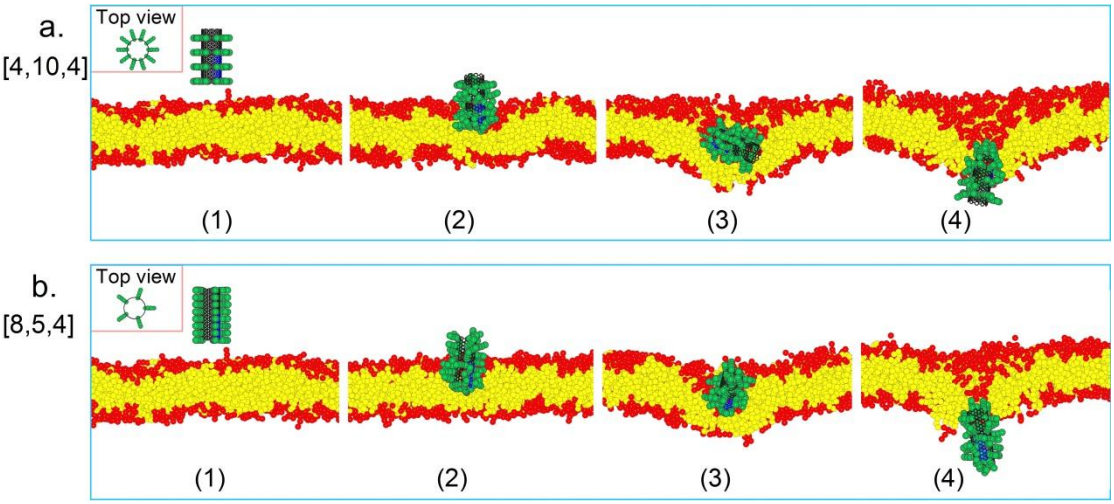

Figure 5

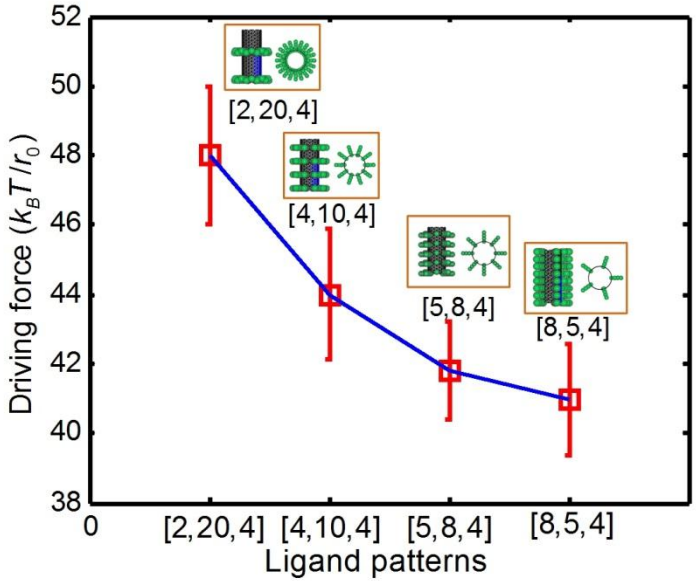

Figure 6

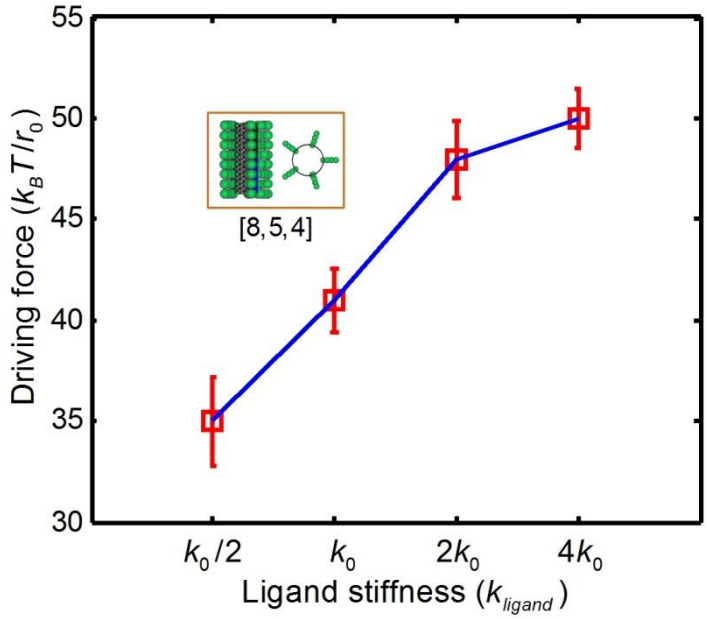

Figure 7

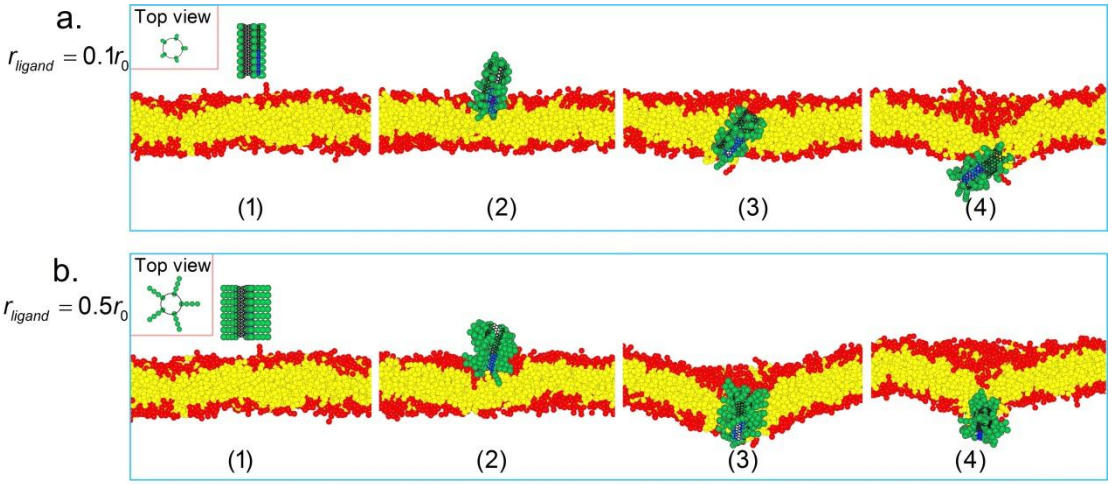

Figure 8

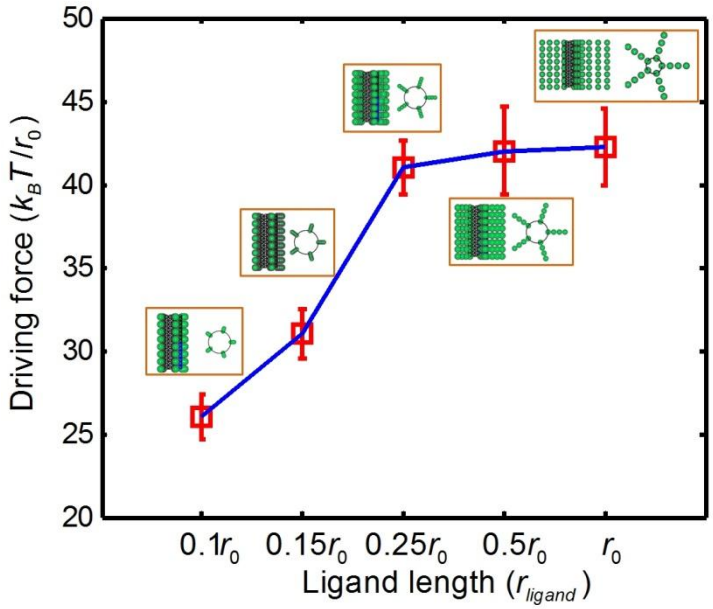

Figure 9

hydrophobic